BLE-based Relative Positioning in the Context of Targeted Bike-to-Everything (B2X) Communication

BEERD VAN DE STREEK, University of Twente, The Netherlands

This paper investigates the feasibility of BLE-based relative positioning for targeted B2X communication. Using Angle of Arrival (AoA) together with BLE communication allows bicycles to determine the location of surrounding devices, enabling focused messages instead of constant broadcasts, potentially improving safety and awareness in urban traffic scenarios. This research builds upon existing projects like E-bell, which focuses on general communication in cycling environments. The paper explores the results of the investigations into antenna placement with respect to obstacles and analyzes how varying bicycle speeds influence AoA estimation effectiveness within a B2X communication system. It shows that obstacles in the environment greatly impact AoA accuracy.

Additional Key Words and Phrases: Bluetooth Low Energy (BLE), Angle of Arrival (AoA), Relative positioning, Bike-to-Everything (B2X) communication

1 INTRODUCTION

The increasing popularity of cycling in urban environments has driven a demand for smarter infrastructure that enhances cyclist safety and promotes a more connected transportation ecosystem. Targeted Bike-to-Infrastructure Communication (B2X) represents a key innovation in this space. By leveraging technologies like Bluetooth Low Energy (BLE) and Angle of Arrival (AoA), B2X allows bicycles to exchange data with surrounding infrastructure, such as traffic lights, and other vehicles, including fellow bikes and even cars. This data exchange, enriched by AoA data, can not only be used to communicate but also to increase cyclists' safety.

Precise relative positioning between bicycles and infrastructure allows for targeted warnings and alerts. Imagine roadside units notifying cyclists of upcoming hazards only when they are in close proximity, reducing broadcast messages that cause information overload and improving reaction times.

By determining cyclists' relative position, the system can tailor message frequency to the specific scenario. Cyclists approaching an intersection might need to receive information more frequently compared to those riding on a straight path. This targeted approach ensures cyclists receive the most relevant messages at the right time.

This paper investigates the accuracy of AoA estimation in various environments. The results show that obstacles in the environment can have a significant impact on the calculated angle, resulting in a less accurate result.

This paper also shows that, in the simulated circumstances, interference and noise induced by bicycle speed do not have a considerable influence on the calculated angle.

TScIT 41, July 5, 2024, Enschede, The Netherlands

1.1 Research Questions

- **RQ1**: How can the accuracy of relative positioning using BLE and AoA be improved in the context of B2X communication?

This research question can be answered using the following subquestions:

- **RQ2**: How does the presence of obstacles in the environment affect the accuracy of BLE-based relative positioning, and how does antenna placement mitigate these effects?
- **RQ3**: How does bicycle speed affect relative positioning accuracy in a B2X network?

2 RELATED WORK

Existing research on B2X communication has focused on data communication protocols [1, 6]. In this research, the performance of communication protocols are evaluated and sometimes compared. Research has also been done on cooperative bicycle localization [12]. However, even though this research involves using BLE signals to detect a bicycle, it focuses more on finding the absolute position of the bicycle with a Global Position System (GPS) sensor. Existing research on BLE and AoA-based (relative) positioning has primarily focused on indoor localization systems, as evidenced by studies like [7, 8, 13]. Often, these studies rely on idealized environments with minimal obstacles, which limits their applicability to real-world scenarios with greater environmental complexity. Other work focuses more on the theoretical possibilities of this subject [15]. This research aims to bridge this gap by investigating the practical effectiveness of BLE and AoA for relative positioning in outdoor environments, where factors like multipath propagation and signal attenuation due to obstacles in the environment can significantly impact accuracy.

3 METHODS

This section describes the fundamentals of relative positioning using BLE AoA

3.1 Angle of arrival

To find the origin of a signal at the receiver side, its angle of arrival can be determined. BLE packets can be equipped with a Constant Tone Extension (CTE) [3]. This CTE is added at the very end of the packet and consists of unmodulated bits, typically all ones. This results in a stable, unchanging signal of 16-160μs.

The receiver side utilizes an antenna array of which the dimensions are known. During reception, the receiver switches between those antennas, sampling parts of the CTE. Due to the physical separation of the antennas and the direction of the incoming signal, the phase of the received CTE shifts between each antenna. By analyzing the phase differences between the samples captured by each antenna, the receiver can extract valuable information about the angle of the incoming signal.

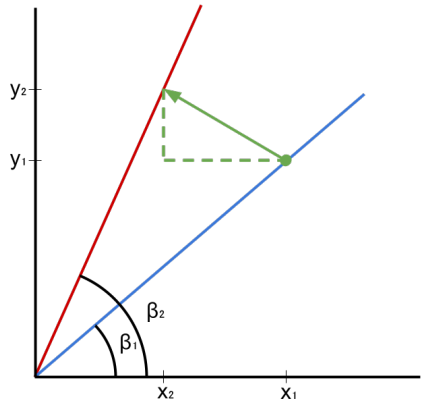

Fig. 1. Position calculation

3.2 Position calculation

Two angle measurements, the time difference, and the vehicle speed and direction can be used to estimate its position relative to the observer. The red and blue lines in Fig. 1 are described using the following formulas

$$y_1 = \tan \beta_1$$
$$y_2 = \tan \beta_2$$

Where β_1 and β_2 are the first and second angle measurements respectively. The velocity components (green lines) are calculated using

$$x_2 = x_1 + v_x \Delta t$$
$$y_2 = y_1 + v_y \Delta t$$

Combining these gives

$$y_2 - y_1 = x_2 \tan \beta_2 - x_1 \tan \beta_1$$

This simplifies to

$$x_2 = \frac{v_x \tan \beta_2 - v_y}{\tan \beta_1 - \tan \beta_2}$$
$$y_2 = x_2 \tan \beta_2$$

3.2.1 Limitations. Complex environments, such as city junctions, are more complicated using this approach. A scene with more interfering objects results in multiple signal paths, introducing more constructive and destructive interference, making it more difficult to determine the signal traveling along the Line of Sight (LoS) path. The calculated angle is then calculated as the angle at which the strongest signals come in at the receiver instead of the real angle between the sender and the receiver. An inaccurate angle measurement will result in an incorrect position estimation.

4 SIMULATION

To get consistent results, a simulation setup was developed using MATLAB®. The advantage of a simulation is that it allows for easy repetition and analysis.

4.1 Simulation setup

For ease of use, the simulation was designed with a modular architecture. This allows for easy switches between different virtual environments and virtual antenna locations.

4.1.1 Environment setup. To simulate an environment as close to a city as possible, a 3d model of a city junction was created using Blender. Blender is open-source 3d software. This 3d model was exported to a Graphics Library Transmission Format (glTF) file. glTF was chosen, because it supports importing materials in MATLAB®. Naming a material as one of the supported MATLAB® materials in Blender ensures that an object is imported and treated that way in the simulation [4, 5]. In MATLAB®, the model is loaded with the `siteviewer` function on line 1. A transmitter and receiver antenna can then be added to this site as is done on lines 5 and 8. The coordinates that are used in `AntennaPosition` are relative to the origin of the virtual environment. The propagation model is then defined on line 11. The maximum number of reflections and diffractions were set to 2 and 1 respectively. Using a higher value will increase the amount of rays calculated, but also increase the time it takes to compute.

```
1  viewer = siteviewer( ...
2      SceneModel="model.gltf", ...
3      ShowEdges=false);
4
5  tx = txsite("cartesian", ...
6      AntennaPosition=[6.1; 0.1; 0.5], ...
7      TransmitterFrequency=2.49e9);
8  rx = rxsite("cartesian", ...
9      AntennaPosition=[0.7; -18.57; 2*pi]);
10
11 pm = propagationModel( ...
12     "raytracing", ...
13     CoordinateSystem="cartesian", ...
14     MaxNumReflections=2, ...
15     MaxNumDiffractions=1);
```

Fig. 2 shows the line-of-sight path between the tx (red) and rx (blue) antennas. The green part of the path indicates the part where a Radio Frequency (RF) signal will be able to travel. The red part indicates that no signal will be able to travel there directly. In this specific case, there is no direct path for the signal to travel to the receiver. The signal can only travel from the sender to the receiver by reflecting off or diffracting around an object in the environment as described in [2, 10]. To model the propagation of the RF signal, ray tracing is used to simulate this behavior [14].

4.1.2 Signal propagation. Ray tracing simulates the way an RF signal travels through the scene, bouncing the signal off objects and calculating the path losses of each ray in the process. This is done using the MATLAB® `raytrace()` function on line 1. A `RayTracingChannel` is then created from these rays on line 3. This is used to simulate a waveform passing through the calculated rays. The sample rate is set to $8 * 1.000.000 = 8MHz$, which is the transfer speed of Bluetooth multiplied by the samples per symbol. This value is high enough to conserve the necessary details of the waveform.

Fig. 2. Line-of-Sight path between the tx and rx antennas

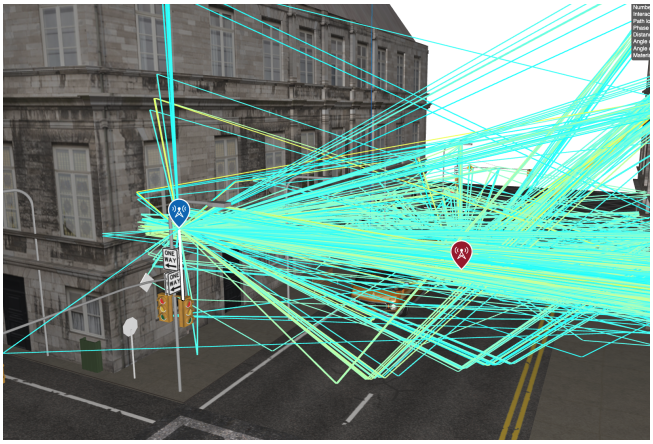

Fig. 3. Resulting signal paths after ray tracing

```
rays = raytrace(tx, rx, pm, Type="pathloss");

channel = comm.RayTracingChannel( ...
    rays, ...
    tx, ...
    rx);
channel.SampleRate = 8*1e6;
```

Fig. 3 shows the resulting rays.

4.1.3 BLE direction-finding packet waveform. As described in subsection 3.1, BLE uses a special type of packet with a CTE. For this, the MATLAB® function `helperBLEGenerateDFPDU` was used. To be able to send this signal over the modeled channel, it is converted to a waveform on line 9.

```
data = helperBLEGenerateDFPDU( ...
    "ConnectionlessCTE", ...
    160, ...
    0:0, ...
    2, ...
    "555551");

accessAddress = int2bit(19088743, 32, false);
waveform = bleWaveformGenerator( ...
    data, ...
    "Mode", "LE1M", ...
    "SamplesPerSymbol", 8, ...
    "ChannelIndex", 1, ...
    "DFPacketType", "ConnectionlessCTE", ...
    "AccessAddress", accessAddress);
```

4.1.4 Signal processing. Now that the waveform is generated, it can be passed through the `RayTracingChannel` to simulate the RF signal propagation. To do this, the `channel` variable that was assigned earlier is used as a function on line 1. Several factors create noise and will alter the waveform, especially in busy environments with a lot of other signals. To simulate this, the resulting waveform is passed through the function `awgn` on line 3 to add additive white Gaussian noise to the signal. To simulate the signal reception with an antenna array, an antenna configuration was defined on line 5 and used by the helper function `helperBLESteerSwitchAntenna` on line 10 which MATLAB® provides as an example. This function is used to simulate the antenna steering and switching.

```
waveform = channel(waveform);

waveform = awgn(waveform, snr, "measured");

cfg = bleAngleEstimateConfig( ...
    "ArraySize", 16, ...
    "ElementSpacing", 0.5, ...
    "SlotDuration", 2, ...
    "SwitchingPattern", 1:16);
waveform = helperBLESteerSwitchAntenna( ...
    waveform, ...
    rays.AngleOfArrival, ...
    "LE1M", ...
    8, ...
    "ConnectionlessCTE", ...
    2, ...
    cfg);
```

After traveling through the channel, additive white Gaussian noise, and steer switching, the BLE receiver picks up the resulting waveform. The waveform is picked up by the BLE receiver which is configured with settings matching the sent signal. This function results in IQ samples (the in-phase (I) and quadrature (Q) parts of the signal). An estimate of the arrival angle of the signal can then be made from these IQ samples. The function `bleAngleEstimate` results in the estimated angle in degrees.

```
[~, ~, iqsamples] = bleIdealReceiver( ...
    waveform, ...
    "Mode", "LE1M", ...
    "SamplesPerSymbol", 8, ...
    "ChannelIndex", 1, ...
```

```
    "DFPacketType", "ConnectionlessCTE", ...
    "SlotDuration", 2);

calculatedAngle = bleAngleEstimate( ...
    iqsamples, ...
    cfg)
```

4.2 Signal smoothing

Signal smoothing helps to refine the received signal by reducing noise and compensating for environmental distortions. This process enhances the overall performance of the BLE AoA system by providing more accurate and stable angle estimations. To do this, a weighted moving average algorithm was implemented as shown below. A weight is assigned to each data point. A window then slides over the values, saving the weighted average of all values in that window.

```
function res = wma(data, weights, windowSize)
    res = zeros(1, length(data));
    for i = 1:length(data)
        if (i < windowSize + 1)
            window = i;
        else
            window = windowSize;
        end
        totalWeight = 0;
        dataPoint = 0;
        for j = 0:window - 1
            dataPoint = dataPoint + ...
                weights(i - j) * data(i - j);
            totalWeight = ...
                totalWeight + weights(i - j);
        end
        res(i) = dataPoint / totalWeight;
    end
end
```

4.3 Obstacles in the environment & antenna placement

To answer RQ2, two 3d scenarios were considered. Antennas were placed at multiple locations in each environment and ray tracing was performed as described above for each receiver antenna separately. To prevent extremely long computation times, the different scenes were kept as simple as possible. After the ray tracing, the signal propagation, signal processing, and angle estimation are performed 100 times for each antenna. The angle error is calculated for each iteration and the mean and standard deviation are saved.

4.3.1 City junction. Scenario 1, as shown in Fig. 4, represents a city junction[1]. It has buildings on both sides of the road and a car. The antennas are placed behind a building or a vehicle, and some of them have line-of-sight. The most important aspect of this scene is the two opposing buildings. These block the LoS for some antennas, providing insight into what happens with the signal after reflecting and diffracting before it is received. This scene is used to simulate the most important aspects of a city environment

[1]Note that this is a simplified visualization. The simulation was performed with more receiver antennas.

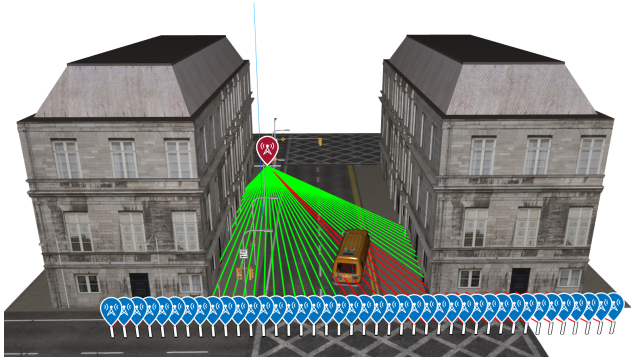

Fig. 4. Scenario 1: A city junction with buildings on opposing sides and a car blocking LoS. Red line parts represent obstructed visibility

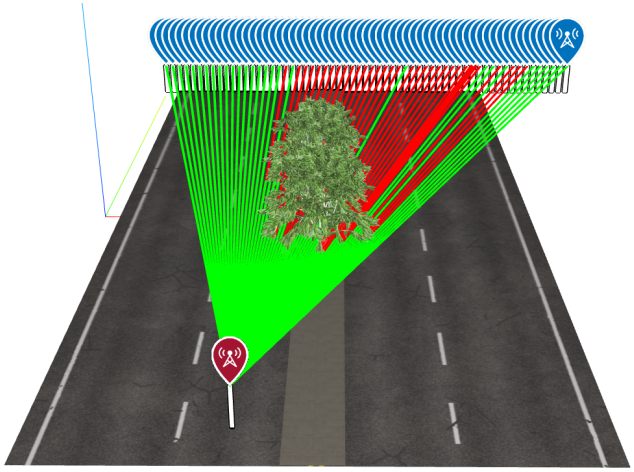

Fig. 5. Scenario 2: A road with vegetation blocking LoS. Red line parts represent obstructed visibility

4.3.2 Vegetation. Scenario 2, as shown in Fig. 5, is a scene with two trees between the sender and the receiver[2]. The trees are marked as 'vegetation', so they are treated as such in the simulation. Note that some of the antennas have a LoS path, exactly going past any branches or leaves. Due to the large amount of leaves in the scene, calculating the rays takes a relatively long time. The most important aspect of this scene is the impact that vegetation might have on the signals, providing insight into what happens when a ray experiences interference from a significant amount of other rays, all traveling in a slightly different direction due to a large number of reflections.

4.4 Bicycle speed

To answer RQ3, the scene was further simplified. The two most dominant paths are selected from the calculated rays after the ray tracing. In most cases, these are the LoS and ground-reflection paths.

[2]See footnote 1

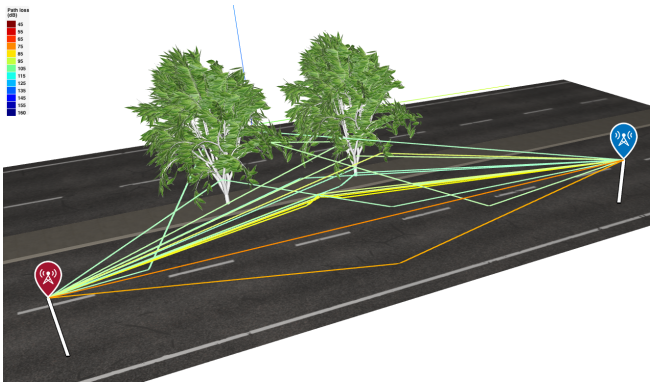

Fig. 6. Dominant paths

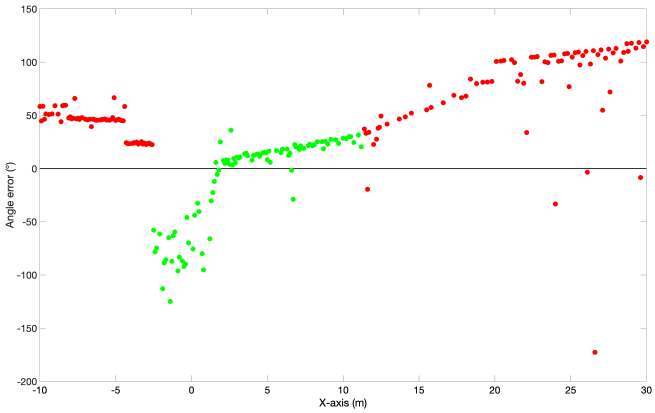

Fig. 7. Scenario 1: Angle error for each antenna before filtering. Green and red data points represent measurements with and without a direct LoS respectively.

The example in Fig. 6 shows that these paths have the least path loss.

The simulation is performed for each speed from 0m/s to 10m/s, which is 36km/h, with 0.1m/s steps.

5 RESULTS

5.1 The effect of obstacles on the angle accuracy

5.1.1 Scenario 1. The results of the simulation for scenario 1 as described in 4.3.1 are depicted in Fig. 8. Roughly the part where the X-position of the receiver is less than -3m and the part where the X-position is higher than 11m are the measurements from the antennas behind the left and right buildings, respectively. These parts do not have a LoS path for the signal to travel, this explains the elevated angle error.

Comparing the raw data in Fig. 7 to the filtered data in Fig. 8 gives some insight into the difference between the raw results and the results that are filtered by the weighted moving average function as described in Section 4.2. The filtered measurements show fewer outliers in the angle errors.

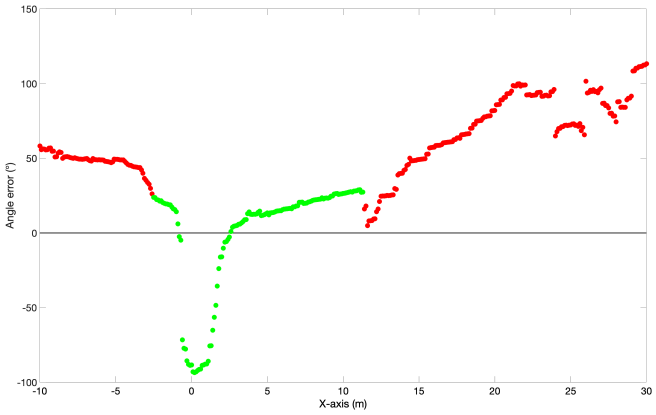

Fig. 8. Scenario 1: Angle error for each antenna after filtering. Green and red data points represent measurements with and without a direct LoS respectively.

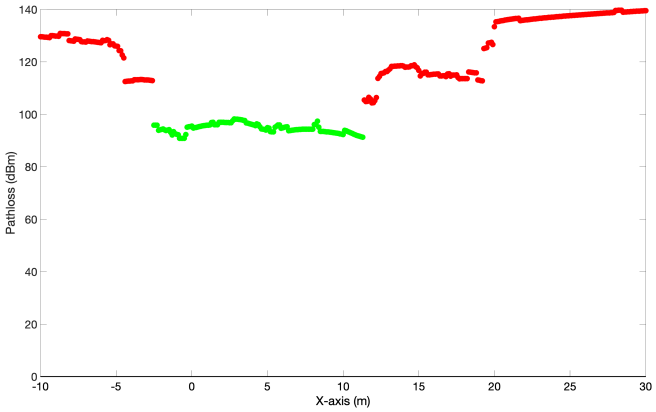

Fig. 9. Scenario 1: Pathloss. Green and red data points represent measurements with and without a direct LoS respectively.

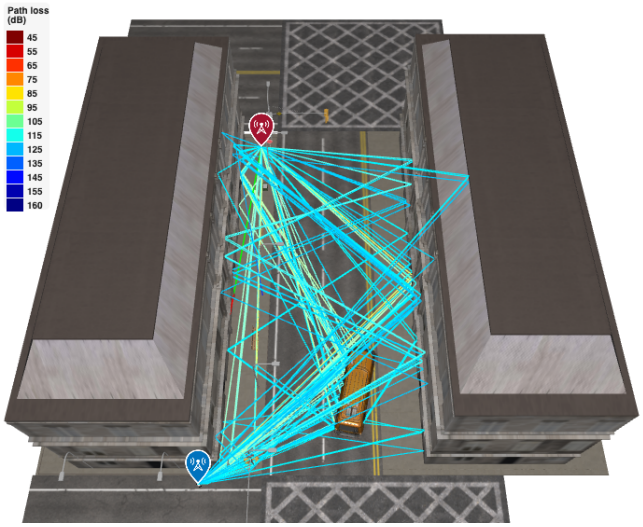

Fig. 10. Scenario 1: Single result at $x = -5$

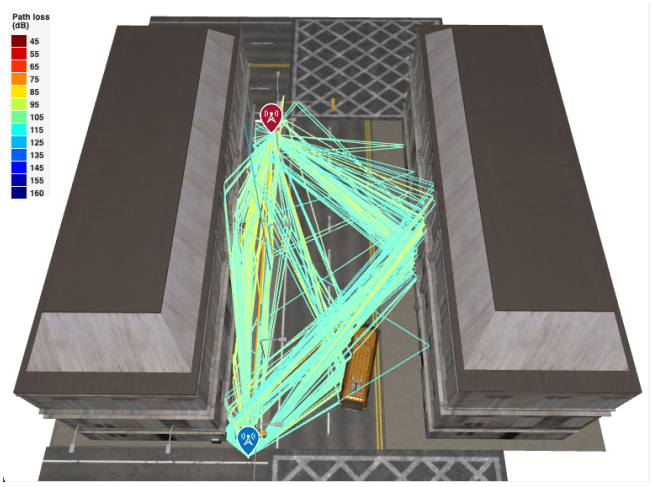

Fig. 11. Scenario 1: Single result at $x = 0$

Investigating a single measurement at $x = -5$ gives the result as shown in Fig. 10. The graph indicates an angle error of ±50°, which is the general angle at which the rays come in at the receiver relative to the LoS. The graph shows that the receiver is able to receive the data even when it is behind a building. The path loss is high due to reflections and diffraction, resulting in a weaker signal at the receiver behind the building.

The green points represent the measurements where a LoS path is available. Remarkably, the angle error increases here. This can be explained by looking at the calculated rays at $x = 0$ in Fig. 11. Here it is clear that the rays come in from a wider range of angles, each with a relatively low path loss, creating more noise at the receiver, and resulting in less accurate measurements.

5.1.2 Scenario 2. The results of the simulation for scenario 2 as described in 4.3.2 are depicted in Fig. 13. The measurements from $x = 0$ to $x = 7$ are stable. However, the closer the paths pass the trees, the more influence the reflections have coming from the trees, resulting in a signal with more noise. This results in a less accurate angle measurement. Fig. 14 shows the pathloss in dBm for each antenna position. It is clear that the pathloss is higher and more variable at the positions at which there is no LoS.

Comparing the data in Fig. 12 and Fig. 13, it is clear that some outliers can be avoided by looking at a couple of earlier data points. Also, the occasional points where a LoS is available (e.g. at $x = 18$ and $x = 24$) prove to be more accurate as the angle error is closer to 0 after filtering.

5.2 The effect of velocity on the angle accuracy

As described in 4.4, the simulation was repeated for different speeds, while keeping every other factor the same, making the vehicle's velocity the only changing factor. This changing velocity did not influence the calculated angle.

However, it must be noted that in practice velocity will influence the calculated angle. As the sender and receiver move, the environment that the signals propagate through changes more quickly. If

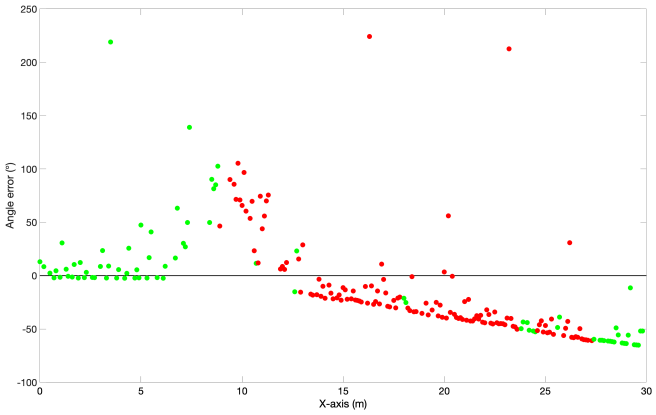

Fig. 12. Scenario 2: Angle error for each antenna before filtering. Green and red data points represent measurements with and without a direct LoS respectively.

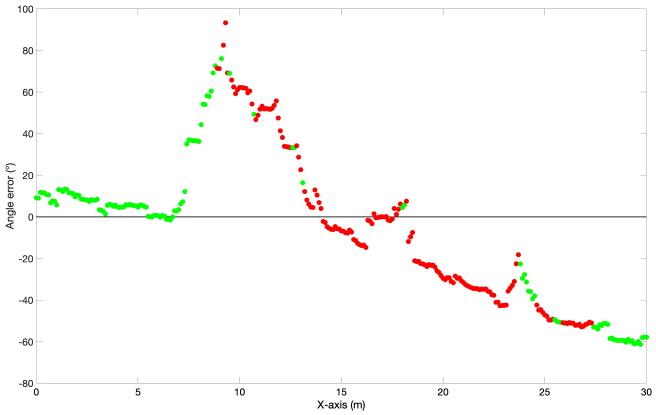

Fig. 13. Scenario 2: Angle error for each antenna after filtering. Green and red data points represent measurements with and without a direct LoS respectively.

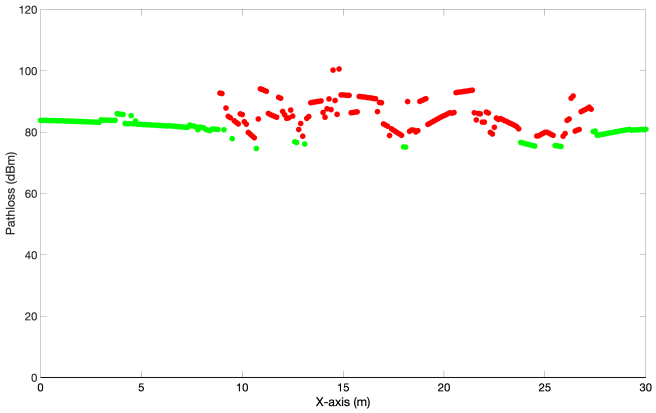

Fig. 14. Scenario 2: Pathloss. Green and red data points represent measurements with and without a direct LoS respectively.

the message frequency is not increased proportionally to the vehicle's velocity, this results in fewer angle measurements for the same distance. In the best case, more measurements with LoS are done, causing the angles to be more precise. In the worst case, it may miss measurements with LoS, leading to a negative impact on the measurements.

6 CONCLUSION

In simple environments, the line-of-sight and ground-reflection are the dominant paths. However, taking buildings, other vehicles, vegetation, street lighting, etc. into account, the scene gets more complex. Measurements taken with a direct line of sight (LoS) and no nearby obstructions are very stable. However, objects in the scene can disrupt this stability by reflecting the signal, altering its original path, and thereby affecting the calculated angle of arrival.

To minimize the impact of small disruptions in the signal, such as those caused by street lighting for example, a weighted moving average algorithm can be used, with the signal strength used as weight.

Overall, 95% of the performed measurements have a $\leq 90^\circ$ error on the real angle between the antennas, even though there are obstacles in the scene. To get the most accurate results, the antennas mustn't be placed close to another object that reflects the signals.

In this context, sender or receiver velocity alone does not influence the angle accuracy. The environment that changes more quickly concerning the sender or receiver has a greater impact. Since the signal is traveling at the speed of light (c), the speed of the sender or receiver can be neglected. This way, measurements at single points will yield the same result as continuous and moving targets.

These insights can be used at future research on this topic as described in Section 7.3

7 DISCUSSION

7.1 Hardware

An initial attempt was performed to answer these research questions through system implementation and real-world experiments. However, finding the right hardware to do this in real life proved to be hard. An nRF5340, specifically the development board from Nordic Semiconductor, was used because of its direction-finding capabilities [11]. However, an external antenna array was needed for this setup to be able to perform direction finding using AoA. The delivered antenna did not contain a suitable cable to connect it to the development board. Due to delivery times, the choice was made to continue the research by performing simulations.

7.2 3D environments

7.2.1 Materials. The materials used in the simulations were quite simple. MATLAB® supports a limited set of materials that can be used in the simulation [4]. Using more realistic materials might influence the outcome of the simulation.

7.2.2 Propagation through objects. Signals are able to pass through materials to a certain extent [9]. This was not considered in the simulations that were performed for this research as only the outside of the 3D models was modelled.

7.2.3 Computational requirements. Ray tracing is a computationally expensive task. Using the MATLAB® Parallel Computing Toolbox makes it possible to perform multiple iterations at once. However, code adjustments must be made to make this possible. Matlab also supports running simulations on computer clusters. This allows the simulations to run more rapidly, enabling faster research iterations.

7.3 Future work

While the simulations conducted in this research have provided valuable insights into improving the accuracy of BLE Angle of Arrival (AoA) systems, it is essential to validate these findings in real-world scenarios. Simulations, while powerful, cannot fully capture the complexity and variability of actual environments. Factors such as interference from other devices or materials, and the dynamic nature of real-world settings can significantly impact signal behavior.

Future research should focus on implementing these techniques in real environments. This will allow to observe the effects that the real world has on the signals and refine the methods accordingly. The insights gained from real-world research will bridge the gap between the theory and actual implementation.

8 ACKNOWLEDGEMENTS

8.1 Use of artificial intelligence

During the preparation of this work, the author used MATLAB AI Chat Playground in order to learn how to use MATLAB®, understand the workings of functions, and help debug code. Also, Grammarly was used for spell-checking. After using these tools/services, the author reviewed and edited the content as needed and takes full responsibility for the content of the work.

8.2 Supervisor

I would like to thank my supervisor, Khalil Ben Fredj, for their expert guidance and support throughout this research. This work would not have been possible without their invaluable insights and encouragement.

REFERENCES

[1] Chaeriah Bin Ali Wael et al. "Analysis of IEEE 802.11p MAC Protocol for Safety Message Broadcast in V2V Communication". In: *2020 International Conference on Radar, Antenna, Microwave, Electronics, and Telecommunications (ICRAMET)*. 2020 International Conference on Radar, Antenna, Microwave, Electronics, and Telecommunications (ICRAMET). Nov. 2020, pp. 320–324. DOI: 10.1109/ICRAMET51080.2020.9298654.

[2] Christopher John Coleman. *Analysis and Modeling of Radio Wave Propagation*. Google-Books-ID: KhPFDQAAQBAJ. Cambridge University Press, Jan. 5, 2017. 492 pp. ISBN: 978-1-316-81307-2.

[3] *Core Specification*. Bluetooth® Technology Website. Jan. 8, 2021. URL: https://www.bluetooth.com/specifications/specs/core-specification-5-1/ (visited on 06/17/2024).

[4] *Create Site Viewer - MATLAB - MathWorks Benelux*. URL: https://nl.mathworks.com/help/antenna/ref/siteviewer.html#mw_ee7e2fef-52ae-4619-83b6-37f2861545be (visited on 06/17/2024).

[5] "Effects of building materials and structures on radiowave propagation above about 100 MHz". In: *Geneva* (Aug. 2023). URL: https://www.itu.int/rec/R-REC-P.2040-3-202308-I.

[6] Noureldin Elhusseiny, Mohamed Sabry, and Hassan Soubra. "B2X Multiprotocol Secure Communication System for Smart Autonomous Bikes". In: *2023 IEEE Conference on Power Electronics and Renewable Energy (CPERE)*. 2023 IEEE Conference on Power Electronics and Renewable Energy (CPERE). Feb. 2023, pp. 1–6. DOI: 10.1109/CPERE56564.2023.10119631.

[7] Shuai He, Hang Long, and Wei Zhang. "Multi-antenna Array-based AoA Estimation Using Bluetooth Low Energy for Indoor Positioning". In: *2021 7th International Conference on Computer and Communications (ICCC)*. 2021 7th International Conference on Computer and Communications (ICCC). Dec. 2021, pp. 2160–2164. DOI: 10.1109/ICCC54389.2021.9674235.

[8] Myungin Ji et al. "Analysis of positioning accuracy corresponding to the number of BLE beacons in indoor positioning system". In: *2015 17th International Conference on Advanced Communication Technology (ICACT)*. 2015 17th International Conference on Advanced Communication Technology (ICACT). ISSN: 1738-9445. July 2015, pp. 92–95. DOI: 10.1109/ICACT.2015.7224764.

[9] Byung-Wan Jo, Jung-Hoon Park, and Kwang-Won Yoon. "The Experimental Study on Concrete Permeability of Wireless Communication Module Embedded in Reinforced Concrete Structures". In: *International Journal of Distributed Sensor Networks* 9.6 (June 1, 2013). Publisher: SAGE Publications, p. 520507. ISSN: 1550-1329. DOI: 10.1155/2013/520507. URL: https://doi.org/10.1155/2013/520507.

[10] Joseph B. Keller. "Geometrical Theory of Diffraction*". In: *Journal of the Optical Society of America* 52.2 (Feb. 1, 1962), p. 116. ISSN: 0030-3941. DOI: 10.1364/JOSA.52.000116. URL: https://opg.optica.org/abstract.cfm?URI=josa-52-2-116 (visited on 06/19/2024).

[11] *nRF5340 Product Specification*. URL: https://docs.nordicsemi.com/bundle/ps_nrf5340/page/keyfeatures_html5.html (visited on 06/17/2024).

[12] Pedro M. Santos et al. "Cooperative Bicycle Localization System via Ad Hoc Bluetooth Networks". In: *2020 IEEE Vehicular Networking Conference (VNC)*. 2020 IEEE Vehicular Networking Conference (VNC). ISSN: 2157-9865. Dec. 2020, pp. 1–4. DOI: 10.1109/VNC51378.2020.9318328.

[13] Adam Satan. "Bluetooth-based indoor navigation mobile system". In: *2018 19th International Carpathian Control Conference (ICCC)*. 2018 19th International Carpathian Control Conference (ICCC). May 2018, pp. 332–337. DOI: 10.1109/CarpathianCC.2018.8399651.

[14] Zhengqing Yun and Magdy F. Iskander. "Ray Tracing for Radio Propagation Modeling: Principles and Applications". In: *IEEE Access* 3 (2015), pp. 1089–1100. ISSN: 2169-3536. DOI: 10.1109/ACCESS.2015.2453991.

[15] Jeroen Zwiers. "BLE-based Relative Positioning in the Context of Targeted Bike-to-Vehicle (B2V) Communication". In: (2023).